


LETTER TO THE EDITOR

Open Access



Stem cell-derived co-grafts contribute to retinal reconstruction and visual functional improvement in a laser damaged rat model

Deepthi S. Rajendran Nair¹, Magdalene J. Seiler^{2,3}, Juan Carlos Martinez-Camarillo^{1,4}, Yuntian Xue^{3,5}, Ruchi Sharma⁶, Kapil Bharti⁶, Mark S. Humayun^{1,4} and Biju B. Thomas^{1,4*} 

Keywords Stem cell-based therapy, Retinal organoids, Retina laser damage, Retinal degenerative disease, Retinal pigment epithelium, Retinal transplantation, Co-graft

Dear Editor,

Irreversible retinal damage can occur due to retinal degenerative (RD) diseases as well as injuries caused by accidents or devices. Laser devices can inflict permanent damage to the retina, leading to the loss of photoreceptors (PRs) and underlying retinal pigment epithelium (RPE), culminating in vision impairment. Since there is no effective treatment for permanent retinal injuries, replacing damaged PRs and RPE with corresponding healthy cells can be a suitable therapeutic approach.

Although various transplantation approaches were demonstrated in congenital RD disease models [1, 2], for the first time we used a novel tissue-engineered co-graft made of RPE and retinal organoid (RO) sheets (Fig. 1; Additional file 1: Figs. S1, S2) to treat laser-damaged

retinal injuries (Fig. 1a; Additional file 1: Materials and methods). Athymic nude rat retinas were exposed to green diode laser (IRIDEX IQ 532) photocoagulation (50–80 mW) in the left eyes in an area approximately the size of the co-grafts (0.4 mm×0.9 mm) (Additional file 1: Fig. S3). Athymic nude rats were used to minimize the possible immunological issues related to the use of human derived RPE and RO sheets for transplantation. Co-grafts were made of human embryonic stem cell (hESC) derived RO sheets dissected from 90 to 110-day-old ROs (Fig. 1b, f; Additional file 1: Figs. S1, S2) and induced pluripotent stem cell (iPSC)-derived RPE cells grown as a monolayer on vitronectin-coated ultrathin parylene membrane [3] (Fig. 1c, d, f). Previously, we had used different bioadhesives to combine RPE monolayer and RO sheets, including matrigel, gelatin, Col-Tgel, and medium viscosity G (MVG) alginate [4]. Considering the rigidity and adhesion property constraints associated with these materials, we used a new approach here based on fibrin glue as the bioadhesive [5]. The co-grafts were transplanted into the subretinal space of athymic nude rats in the laser-damaged area using a specially designed tool (Fig. 1e) that enabled precise graft placement (Fig. 1f–h). Post-surgical optical coherence tomography (OCT) imaging confirmed the subretinal placement (Fig. 1j) of the grafts and its growth and maturation were monitored until 7 months. Visual functional benefits were measured periodically using optokinetic nystagmus (OKN) testing and electroretinogram (ERG) recording.

*Correspondence:

Biju B. Thomas
biju.thomas@med.usc.edu

¹ Department of Ophthalmology, USC Roski Eye Institute, University of Southern California, Los Angeles, CA 91030, USA

² Departments of Physical Medicine and Rehabilitation, Ophthalmology, Anatomy, and Neurobiology, University of California, Irvine, Irvine, CA 92697, USA

³ Stem Cell Research Center, University of California, Irvine, Irvine, CA 92697, USA

⁴ USC Ginsburg Institute for Biomedical Therapeutics, University of Southern California, Los Angeles, CA 90033, USA

⁵ Biomedical Engineering, University of California, Irvine, Irvine, CA 92617, USA

⁶ Unit on Ocular and Stem Cell Translational Research, National Eye Institute, NIH, Bethesda, MD 20892, USA



© The Author(s) 2025. **Open Access** This article is licensed under a Creative Commons Attribution 4.0 International License, which permits use, sharing, adaptation, distribution and reproduction in any medium or format, as long as you give appropriate credit to the original author(s) and the source, provide a link to the Creative Commons licence, and indicate if changes were made. The images or other third party material in this article are included in the article's Creative Commons licence, unless indicated otherwise in a credit line to the material. If material is not included in the article's Creative Commons licence and your intended use is not permitted by statutory regulation or exceeds the permitted use, you will need to obtain permission directly from the copyright holder. To view a copy of this licence, visit <http://creativecommons.org/licenses/by/4.0/>. The Creative Commons Public Domain Dedication waiver (<http://creativecommons.org/publicdomain/zero/1.0/>) applies to the data made available in this article, unless otherwise stated in a credit line to the data.

About 7-months post-surgery, electrophysiological mapping of the brain visual center, the superior colliculus (SC), was conducted as a terminal procedure followed by histological examinations.

Histology analysis of laser-injured eyes (Fig. 1i; Additional file 1: Fig. S3) showed significant damage to multiple retinal layers (most importantly PR and RPE). Vertical and horizontal OCT scan images corroborated evidence

of suitable graft placement (Fig. 1j). Distinct structural modifications in the appearance of the co-graft were noticed at various post-surgical time points. Compared to the immediate post-surgery OCT imaging showing a raised and thick appearance, the co-graft appeared more intact at 3- and 6-month (Fig. 1j) time points. In the laser-damaged control rat groups, sham surgery rat groups (Fig. 1k), parylene implanted rat groups and RPE

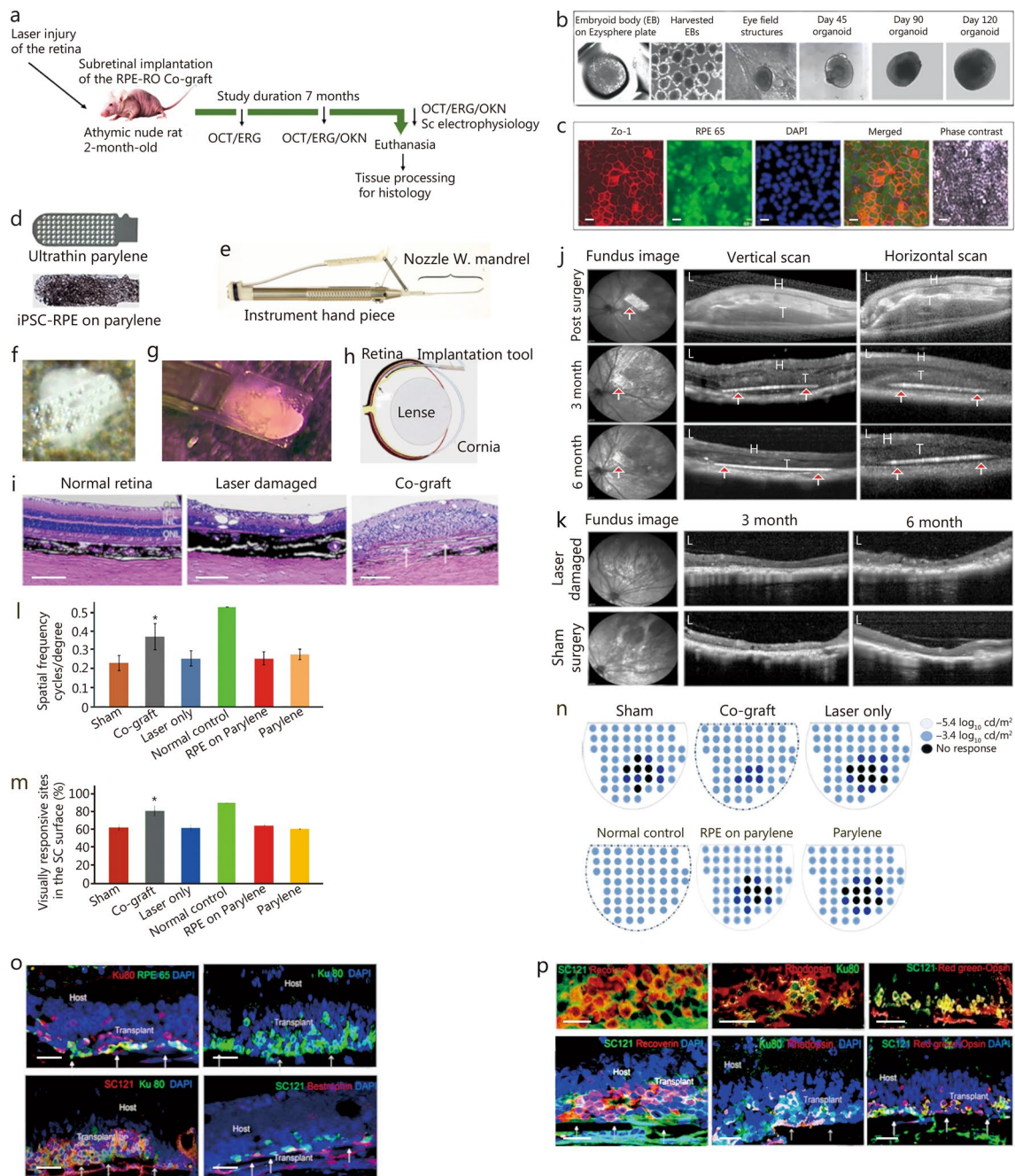


Fig. 1 (See legend on next page.)

(See figure on previous page.)

Fig. 1 Stem cell-derived co-grafts contribute to the retinal reconstruction and visual functional improvement in laser damaged athymic nude rat model. **a** Schematic protocol of the experimental procedures in athymic nude rats with retinal laser injury. **b** Various stages of retina organoid (RO) development-embryoid body on EZSPHERE plate, harvested embryoid bodies in 100 mm plate, eye field structures developed in matrigel coated plates, and ROs at different developmental stages. **c** Induced pluripotent stem cell-derived retinal pigment epithelium (iPSC-RPE) expressing different RPE markers: zonula occludens-1 (Zo-1), retinal pigment epithelium-specific 65 kD protein (RPE 65), nuclear stain DAPI, and phase contrast image of iPSC-RPEs. Scale bar = 50 μ m. **d** Ultrathin parylene membrane before and after culturing of iPSC-RPE monolayer **e** Co-graft implantation tool. **f** Co-graft made of iPSC-RPE and RO sheet using fibrin glue. **g** Co-graft loaded into the nozzle of the implantation tool prior to transplantation. **h** Diagrammatic sketch showing subretinal implantation of the co-graft. **i** Hematoxylin and eosin (HE) stained image of the athymic nude rat retinas. **j** Optical coherence tomography (OCT) imaging of the retina-fundus images showing the co-graft in the vertical, and horizontal scans immediately after the surgery, 3-months post-surgery, and 6-months post-surgery. Hyperreflexion in the OCT images (white arrows with red arrowhead) indicates the subretinal placement of the parylene membrane. H host, T transplant. **k** Fundus image and OCT scanning image of the laser damaged and sham surgery retina showing the retinal thinning that remained unchanged over time. Scale bar = 200 μ m. **l** Optokinetic nystagmus (OKN) testing conducted at 6 month time points. Significant visual improvement in co-graft implanted rats compared to the laser-damaged control rats ($P < 0.05$) was evident at 6 month time point. $*P < 0.05$. **m** Superior colliculus (SC) activities recorded by single electrode mapping showing statistically significant ($P < 0.05$, Student's *t*-test) improvement in visual responses in the co-graft implanted rats compared to the sham surgery group and laser damaged control group. $*P < 0.05$ **n** SC activities recorded by multielectrode array (MEA) mapping at 7 months post-surgery. Laser beams caused a focal retinal injury that resulted in the absence of any visual activity (scotoma) that was partially repaired by co-graft implantation. **o** Confocal images of the immunostained athymic nude rat retinas 7 months post-surgery. Transplanted co-grafts expressed RPE 65 (RPE marker)/DAPI, Ku80 (human nuclear marker)/DAPI, SC121 (human cytoplasmic marker)/Ku80/DAPI, and bestrophin (RPE marker)/Ku80. White arrows denote parylene membrane. **p** Transplanted co-grafts expressing general photoreceptor marker, recoverin, rod specific marker rhodopsin and cone photoreceptor marker, red-green opsin. Scale bar = 100 μ m

on parylene implanted rat groups (Additional file 1: Fig. S4), the thinning of the retina remained unchanged.

The ERG recording failed to detect apparent differences between various experimental groups (Additional file 1: Fig. S5). This can be because of the small size of the laser-damaged area. It is plausible that visual deficit is limited to such a very small area (less than 1 mm) may not be sufficient to cause measurable changes in the ERG signals. OKN measurements showed improvement in visual acuity in co-graft implanted groups compared to the sham group and the control laser-damaged groups at the 6-month time point ($P < 0.05$; Fig. 1l). Single electrode mapping of the SC demonstrated significantly higher number of SC sites responding to light in the co-graft implanted rats ($n = 5$) compared to the sham surgery group ($n = 4$) and the control laser-damaged rats ($n = 2$, $P < 0.05$; Fig. 1m). Corroborating the above observation, spatial properties of the visual responses measured using multielectrode array (MEA) (Fig. 1n; Additional file 1: Fig. S5) demonstrated the absence of scotoma in most of the co-graft implanted rats (3/4). In contrast, the presence of scotoma was evident in all sham surgery rats ($n = 4$), parylene only implanted rats ($n = 1$), parylene + RPE implanted rats ($n = 4$), and control laser damaged rats ($n = 2$; Fig. 1n).

Histological examination of the co-graft transplanted eyes demonstrated the presence of co-grafts containing RPE and RO entities. Immunostaining with human nuclear antigen (Ku80) and cytoplasmic marker (SC121) confirmed that the transplanted cells were of human origin (Fig. 1o). Differentiation of cells inside the co-graft

into PRs was evidenced by the expression of the general PR marker recoverin, as well as specific markers for rods (rhodopsin) and cones (red-green opsin, Fig. 1p). Prevalence of rosette formation of transplanted PRs was mostly absent in these rats compared to our previous studies in which various congenital disease models were used [1, 2, 4]. This can be due to the improved co-graft fabrication technique, although differences between disease models may also play a role. The laser damaged control eyes showed a total absence of RPE and PRs in the laser damaged area 7 months after surgery (Additional file 1: Fig. S3).

The RPE cells in the co-graft in vivo expressed the RPE markers such as bestrophin and RPE 65 (Fig. 1o), suggesting their survival. Synaptophysin, a marker for presynaptic vesicles, exhibited strong staining in both host and transplant, suggesting possible synaptic connections between host and transplant (Additional file 1: Fig. S6). Staining targeting cellular retinaldehyde binding protein, which is specific for Müller cells and RPE, demonstrated the presence of Müller cells within the transplants (Additional file 1). Additionally, the host's Müller cells exhibited a greater degree of reactivity compared to those in the transplant, as indicated by glial fibrillary acidic protein (GFAP) staining (Additional file 1: Fig. S7). Rod bipolar cells [marker: protein kinase C alpha (PKC α)] were also present in the transplant layer (Additional file 1: Fig. S7). Notably, there was no visible presence of fibrin glue, suggesting its complete degradation, enabling integration between the RPE and the organoid sheet. This study presents a

more advanced method to create retinal co-grafts by combining RO sheet and polarized RPE monolayer, with fibrin glue serving as the bioadhesive. The survival and maturation of PRs in the co-graft after transplantation, along with the resulting improvements in visual function, render this technique appropriate for the treatment of permanent retinal injuries.

Co-graft implanted retinas require more extensive studies to better understand morphological integration, outer segment formation, and synaptic connectivity. While no rosette formation was observed, and the transplanted cells were notably preserved, the co-grafts did not fully develop the organized, laminar structure typical of normal retinas. The proximity of transplanted cells to intermediate neurons suggests potential for synaptic connections, although partial disorganization and loss of laminar structure were observed in histological analysis, likely due to the small eye size and xenograft issues in rat models. Further studies focusing on synaptic connectivity are essential, given that cytoplasmic transfer poses a risk associated with photoreceptor transplantation. However, unlike previous studies which used single-cell suspensions derived from primary or progenitor cells that may lead to cytoplasmic transfer [6], the integrity of the co-grafts in this study suggests that this effect is unlikely. Future use of focal electroretinography (ERG) could provide insight into functional differences between damaged and healthy retinal areas, contributing to improved transplant efficiency. This "proof of concept" in immunodeficient rat models marks a significant milestone for tackling advanced retinal degeneration diseases in humans.

This study demonstrates the therapeutic potential of co-grafts composed of retinal organoid (RO) sheets and retinal pigment epithelium (RPE) for retinal reconstruction. Using a laser-damaged rat model, we showed that co-graft implantation improves visual function, highlighting a promising approach for treating retinal injuries and degenerative diseases. The co-graft method, supported by fibrin glue as a bioadhesive, facilitates the survival, maturation, and functional integration of transplanted photoreceptors, enabling synaptic connections with host retinal neurons. Further research in larger animal models is essential to address immune rejection and optimize graft placement, but this work lays an important foundation for translating tissue-engineered retinal therapies into clinical applications targeting vision loss from retinal degeneration.

Abbreviations

CRX	Cone-rod homeobox gene
ERG	Electroretinogram

iPSC	Induced pluripotent stem cells
MEA	Multielectrode array
OCT	Optical coherence tomography
OKN	Optokinetic nystagmus
PR	Photoreceptors
RD	Retinal degenerative
RO	Retinal organoid
RPE	Retinal pigment epithelium
SC	Superior colliculus

Supplementary Information

The online version contains supplementary material available at <https://doi.org/10.1186/s40779-025-00601-7>.

Additional file 1: Materials and methods. Table S1 List of primary antibodies. **Table S2** List of secondary antibodies. **Fig. S1** Characterization of CRX-GFP retinal organoids. **Fig. S2** Preparation of 3D retina organoids for transplantation. **Fig. S3** Optical coherence tomography (OCT) and immunohistochemistry (IHC) of control and laser damaged retinas. **Fig. S4** Optical coherence tomography (OCT) and hematoxylin and eosin (HE) staining of parylene and retinal pigment epithelium (RPE) on parylene implanted retinas. **Fig. S5** Electroretinogram (ERG) data and superior colliculus (SC) electrophysiology setup. **Fig. S6** Transplanted co-grafts expressing recoverin and synaptophysin. **Fig. S7** Transplanted Co-grafts expressing glial fibrillary acidic protein (GFAP)/Ku80 (human nuclear marker), and cellular retinaldehyde binding protein (CRALPB; specific for Müller cells and RPE)/protein kinase C alpha (PKC α ; human specific-Rod bipolar cell marker) after 7 months.

Acknowledgements

The authors thank Majlinda Lako (Newcastle University, United Kingdom) for donating the CRX-GFP human embryonic stem cell line. The authors would also like to thank all past and current students of the Thomas Lab for their research assistance. The authors want to thank Xiaopeng Wang for histology assistance and Ying Lu for assistance with OCT and ERG.

Authors' contributions

BBT and MJS conceptualized and designed the study, provided financial and administrative support, and contributed to the provision of study materials. DSRN, BBT, JCMC, YX, and MJS were responsible for data collection and assembly. DSRN, BBT, KB, RS, and MJS conducted data analysis and interpretation. DSRN, BBT, MJS, RS, and JCMC were involved in writing the manuscript. DSNR, BBT, MJS, YX, JCMC, KB, RS, MSH, and MJS gave final approval of the manuscript. All authors read and approved the final manuscript.

Funding

This work was supported by the National Eye Institute, National Institute of Health, Bethesda, Maryland, USA [CIRM DISC1-09912 (BBT), NIH EY031144 (BBT), R01 EY031834, EY-017337], the USC Ophthalmology Core (NIH P30EY029220, an unrestricted grant to the USC Department of Ophthalmology from RPB), and the BrightFocus Foundation (M2016186, BBT). The authors acknowledge departmental support from a Research to Prevent Blindness (RPB, New York, NY, USA) unrestricted grant to the UCI Department of Ophthalmology.

Availability of data and materials

All data generated or analyzed during this study are included in this published article and its supplementary information file. Further inquiries are available from the corresponding author upon reasonable request.

Declarations

Ethics approval and consent to participate

All experiments were approved by the University of Southern California Institutional Animal Care and Use Committee (IACUC, Protocol No. 21303) and were performed following the National Institutes of Health (NIH) Guide for the Care and Use of Laboratory Animals and the Association for Research in Vision

and Ophthalmology (ARVO) Statement for the Use of Animals in Ophthalmic and Vision Research.

Consent for publication

Not applicable.

Competing interests

Mark S. Humayun is an investor, a consultant, and a board member of Regenerative Patch Technologies (RPT) and holds an RPT patent. The remaining authors declare that the research was conducted in the absence of any commercial or financial relationships that could be construed as a potential conflict of interest. The authors declare that they have no competing interests.

Received: 28 October 2023 Accepted: 5 March 2025

Published online: 21 May 2025

References

1. Lin B, McLelland BT, Aramant RB, Thomas BB, Nistor G, Keirstead HS, et al. Retina organoid transplants develop photoreceptors and improve visual function in RCS rats with RPE dysfunction. *Invest Ophthalmol Vis Sci*. 2020;61(11):34.
2. McLelland BT, Lin B, Mathur A, Aramant RB, Thomas BB, Nistor G, et al. Transplanted hESC-derived retina organoid sheets differentiate, integrate, and improve visual function in retinal degenerate rats. *Invest Ophthalmol Vis Sci*. 2018;59(6):2586–603.
3. Rajendran Nair DS, Zhu D, Sharma R, Martinez Camarillo JC, Bharti K, Hinton DR, et al. Long-term transplant effects of iPSC-RPE monolayer in immunodeficient RCS rats. *Cells*. 2021;10(11):2951.
4. Thomas BB, Lin B, Martinez-Camarillo JC, Zhu D, McLelland BT, Nistor G, et al. Co-grafts of human embryonic stem cell derived retina organoids and retinal pigment epithelium for retinal reconstruction in immunodeficient retinal Degenerate Royal College of Surgeons rats. *Front Neurosci*. 2021;15:752958.
5. Gandhi JK, Mano F, Iezzi R, LoBue SA, Holman BH, Fautsch MP, et al. Fibrin hydrogels are safe, degradable scaffolds for sub-retinal implantation. *PLoS ONE*. 2020;15(1):e0227641.
6. Singh MS, Balmer J, Barnard AR, Aslam SA, Moralli D, Green CM, et al. Transplanted photoreceptor precursors transfer proteins to host photoreceptors by a mechanism of cytoplasmic fusion. *Nat Commun*. 2016;7:13537.